Near-field optical potential for a neutral atom

K. Kobayashi* and S. Sangu
ERATO Localized Photon Project, Japan Science and Technology Corporation, 687-1 Tsuruma, Machida, Tokyo 194-0004, Japan

H. Ito and M. Ohtsu†
Interdisciplinary Graduate School of Science and Engineering, Tokyo Institute of Technology, 4259 Nagatsuta-cho, Midori-ku, Yokohama, Kanagawa 226-8502, Japan

(Received 19 April 2000; published 11 December 2000)

We study an effective interaction potential between a neutral atom and a nanometric probe tip in optical near-field systems. The wave-number dependence of the coupling coefficients of exciton polaritons is described with the effective-mass approximation, where massive virtual photons are exchanged between the atom and the probe tip. The near-field optical potential is shown as the sum of the Yukawa functions with several kinds of effective masses or interaction ranges, and is characterized in terms of detuning for the resonance energies of the atom and the probe tip. Consequently, we find that a potential minimum is produced for a blue detuning case. This result indicates that an atom can be trapped in the near-field optical potential well. Furthermore, we numerically investigate deflection and trapping of a single atom by means of optical near fields generated from a nanometric probe tip. The dependence on the probe-tip size, the kinetic energy of the cold atom, and the excitation energies of both probe tip and atom is clarified.

DOI: 10.1103/PhysRevA.63.013806 PACS number(s): 42.50.Ct, 32.80.Pj

I. INTRODUCTION

Optical near-field techniques are considered promising as enabling technologies for nanostructure fabrication with arbitrary shapes and high spatial accuracy far beyond the diffraction limit [1]. As a result of the development of a highly efficient probe tip for optical near-field systems [2–4], local excitation of a nanometric quantum dot [4–6] and photochemical deposition of, for example, Zn [7,8] and ZnO [1] on a sub-100-nm scale have become possible. The ultimate goal of such fabrication is to make atomic-scale crystal growth by manipulating individual atoms with optical methods [2,9–11]. In fact, an optical near-field probe tip with a diameter of less than 10 nm has been developed and is expected to be used in atom manipulation experiments [2]. Microscopic or quantum-mechanical treatment [12–16] of the interaction between such a nanometric probe tip and an atom is essential for describing the atom manipulation with optical near fields. In particular, it is important to consider the nanometric tip and the atom as an interacting system through the coupling to a macroscopic bath system made up of incident photons, substrate, and/or fiber probe. It should be noted that the conventional theories in near-field optics, which deal with the tip and the atom independently, have been developed in order to analyze scanning-microscope images with *macroscopic* quantities such as refractive indices. Therefore they are not suitable for formulating *microscopic* phenomena associated with optical near-field techniques.

In this paper we concentrate on the theoretical derivation and evaluation of effective interaction potentials between a neutral atom and a nanometric probe tip. We follow the well-known approach of describing atomic behavior in terms of the optical potential, by which we can obtain a clear physical image. This kind of treatment also allows us to quantitatively discuss the interacting system. The near-field optical potential, however, has not been derived yet in a microscopic way. That is the chief reason why we try to microscopically derive the potential.

Although the existing theories have predicted the possibility of atom trapping, they have never included a microscopic and consistent discussion on the near-field optical potential since a nanometric probe tip has not been employed to produce optical near fields. Let us take an example illustrating this point clearly. An approach for atom trapping by evanescent fields has been proposed; it employs two laser beams that propagate through totally internal reflection by a flat prism [17], or by the wall of a microsphere [18]. In this scheme, the blue-detuned beam has a larger incident angle than the red-detuned beam, so that two different evanescent fields with two different penetration depths are produced in a vacuum side. The fundamental idea is based on the potential balance due to the existence of these two fields. This kind of trapping is usually explained with reference to the *far-field* optical potential [19] qualified by the dressed atom theory [20], which is applied to a wide range of phenomena, from atom-photon interaction in general to laser cooling [21]. The optical near field, however, is a highly mixed state with material excitation rather than the propagating light field. This viewpoint becomes more and more important as we consider a tiny generator of the optical near field, whose size is much smaller than the wavelength of light. It has therefore remained an open question whether atomic behavior in near-field optical systems can be adequately expressed by the optical potential borrowed from the far-field theory.

We develop a consistent theory appropriate for investigating the near-field optical manipulation of an atom. The atom is considered to interact with the nanometric probe tip via an

*Electronic address: kkoba@ohtsu.jst.go.jp
†Also at ERATO Localized Photon Project, Japan Science and Technology Corporation.

elementary excitation mode of real photons and the macroscopic matter system. We discuss the possibility of trapping a single atom, giving a numerical estimation of the near-field optical potential. The paper is organized as follows. Section II presents a formulation for the derivation of a near-field optical potential with the help of the projection-operator method. Section III clarifies the fundamental features of the near-field optical potential. In Sec. IV a numerical analysis of atom deflection and trapping is performed. Section V offers some concluding remarks.

II. FORMULATION

It is reasonable to use classical electromagnetic theories for macroscopic descriptions of the behavior of light and matter. However, when the size of the probe tip or aperture becomes nanometric, that is, comparable to an atomic scale, there is no guarantee that we can use classical theories to correctly formulate optical near-field problems such as interactions between atoms or nanometric samples and the probe tip. We therefore try to study the problems within a quantum theoretical framework, paying special attention to the hierarchical structure of optical near-field systems [1,16]. Our formulation is general, but hereafter we focus on an effective interaction between a probe tip and a neutral atom. On the basis of the projection-operator method, the effective interaction can be exactly expressed by using a small number of bases after renormalizing the effects of the other degrees of freedom [see Eqs. (7a) and (7b)]. The renormalizing effects may include cavity quantum-electrodynamic (QED) effects, energy shift and mixing of the ground and higher-level states of the atom, and the probe tip. It is noted that the nanometric probe tip has discrete energy levels. If we employ static or steady states as the bases, the effective interaction corresponds to an effective potential for the relevant system from quantum-field theoretical consideration. The potential picture is very appropriate for investigating atomic behavior, and will be adopted in the following discussion.

In order to derive an effective potential $V_{\mathrm{eff}}(r)$, where r is the atom's position measured from an arbitrary point $(\vec{r}_2)$ inside a probe tip, we divide an optical near-field system into two subsystems: (i) incident propagating light consisting of real photons that interact with a macroscopic matter system, typically a prism in the collection mode or a fiber probe in the illumination mode [2], and (ii) a nanometric probe tip and an atom. Figure 1 illustrates the division considered here. These two subsystems interact with each other, and consequently produce the interaction between the probe tip and the atom in the subsystem (ii). The interaction originates from the exchange of virtual exciton polaritons, as we will see in the following.

The starting point is that the eigenvalues and eigenstates of the total Hamiltonian $\hat{H}$ for the optical near-field system are written as E_λ and $|\Psi_\lambda\rangle$, respectively; that is,

$$\hat{H}|\Psi_\lambda\rangle=(\hat{H}_0+\hat{V})|\Psi_\lambda\rangle=E_\lambda|\Psi_\lambda\rangle, \tag{1}$$

where $\hat{H}_0$ consists of the Hamiltonians $\hat{H}_{\mathrm{bath}}$ for the subsystem (i) and $\hat{H}_A+\hat{H}_B$ for the subsystem (ii), while $\hat{V}$ denotes the interaction between the two subsystems. It is noted that the Hamiltonian $\hat{H}_A$ ($\hat{H}_B$) describes the states of the atom (the probe tip) as an isolated quantum-mechanical system. The suffix λ distinguishes each eigenstate. Defining the projection operators P and $Q=1-P$ in the usual manner as

$$|\Psi_\lambda^{(1)}\rangle=P|\Psi_\lambda\rangle, \quad |\Psi_\lambda^{(2)}\rangle=Q|\Psi_\lambda\rangle, \tag{2a}$$

$$P^2=P, \quad PQ=QP=0, \tag{2b}$$

$$[P,\hat{H}_0]=[Q,\hat{H}_0]=0, \tag{2c}$$

we divide the eigenstates $|\Psi_\lambda\rangle$ into two groups, $|\Psi_\lambda^{(1)}\rangle$ in P space and $|\Psi_\lambda^{(2)}\rangle$ in Q space. By using Eqs. (2a)–(2c), Eq. (1) is then rewritten as a set of equations

$$(E_\lambda-\hat{H}_0)P|\Psi_\lambda^{(1)}\rangle=P\hat{V}P|\Psi_\lambda^{(1)}\rangle+P\hat{V}Q|\Psi_\lambda^{(2)}\rangle, \tag{3a}$$

$$(E_\lambda-\hat{H}_0)Q|\Psi_\lambda^{(2)}\rangle=Q\hat{V}P|\Psi_\lambda^{(1)}\rangle+Q\hat{V}Q|\Psi_\lambda^{(2)}\rangle. \tag{3b}$$

From the above equation Eq. (3b), it is possible to formally express $Q|\Psi_\lambda^{(2)}\rangle$ by $P|\Psi_\lambda^{(1)}\rangle$ as

$$\begin{aligned} Q|\Psi_\lambda^{(2)}\rangle&=(E_\lambda-\hat{H}_0-Q\hat{V})^{-1}Q\hat{V}P|\Psi_\lambda^{(1)}\rangle \\ &=\hat{J}(E_\lambda-\hat{H}_0)^{-1}Q\hat{V}P|\Psi_\lambda^{(1)}\rangle, \end{aligned} \tag{4a}$$

$$\hat{J}=[1-(E_\lambda-\hat{H}_0)^{-1}Q\hat{V}]^{-1}, \tag{4b}$$

and the eigenstates $|\Psi_\lambda\rangle$ for the total Hamiltonian can then be expressed in terms of the eigenstates in P space as

$$|\Psi_\lambda\rangle=(P+Q)|\Psi_\lambda\rangle=\hat{J}P|\Psi_\lambda^{(1)}\rangle. \tag{5}$$

Since both of the states satisfy the normalization condition, we can rewrite this as

$$|\Psi_\lambda\rangle=\hat{J}P(P\hat{J}^\dagger\hat{J}P)^{-1/2}|\Psi_\lambda^{(1)}\rangle. \tag{6}$$

Using the projection operators, we can thus consistently treat the interaction as follows [1,16]:

$$\langle\Psi_\mu|\hat{V}|\Psi_\lambda\rangle=\langle\Psi_\mu^{(1)}|\hat{V}_{\mathrm{eff}}|\Psi_\lambda^{(1)}\rangle, \tag{7a}$$

$$\hat{V}_{\mathrm{eff}}=(P\hat{J}^\dagger\hat{J}P)^{-1/2}(P\hat{J}^\dagger\hat{V}\hat{J}P)(P\hat{J}^\dagger\hat{J}P)^{-1/2}, \tag{7b}$$

where the bare interaction $\hat{V}$ operates on exact states $|\Psi\rangle$ of the total system, while $\hat{V}_{\mathrm{eff}}$ operates on a small number of states $|\Psi^{(1)}\rangle$ of the subsystem (ii).

In order to proceed further in evaluating Eq. (7a), we need explicit forms of $\hat{V}$ and $\hat{J}$ as well as P. First the interaction $\hat{V}$ between the two subsystems is described by the multipolar QED Hamiltonian [22]. We employ, for simplicity, its dipole approximation as

$$\hat{V}=-\sum_\alpha \theta(z_\alpha)\hat{\vec{\mu}}_\alpha\cdot\hat{\vec{D}}(\vec{r}_\alpha), \tag{8}$$

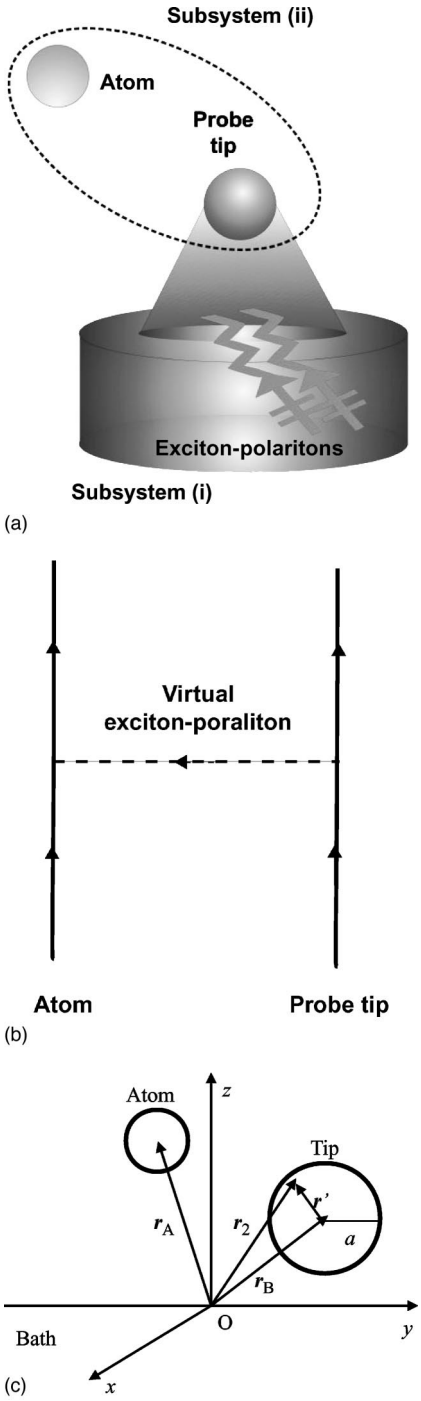

FIG. 1. Schematic illustration of how to divide a near-field optical system. A nanometric probe tip and an atom, referred to as subsystem (ii), are extracted from the total system, while the remaining part is regarded as subsystem (i). These two subsystems interact with each other via an elementary excitation mode, or exciton-polaritons as shown in wavy lines. As a result, the probe tip and the atom also interact by exchanging virtual exciton polaritons. Geometry of the model is also inserted. The vectors $\vec{r}_A$ and $\vec{r}_B$ denote the center of the atom and the center of the tip sphere with a radius of a, respectively. An arbitrary position inside the tip sphere is represented by $\vec{r}_2$ measured from the origin of the coordinates system, and $\vec{r}'$ measured from the center of the tip sphere, respectively.

where $\theta(z)$ and $\hat{\vec{\mu}}(\vec{r})$ are the step function and the dipole operator, respectively. The displacement field operator is denoted as $\hat{\vec{D}}(\vec{r})$, and is given by the conjugate momentum operator $\hat{\vec{\Pi}}(\vec{r})$ of the vector potential operator $\hat{\vec{A}}(\vec{r})$. Then it is necessary to find out an explicit form of the operator $\hat{J}$ that can be handled. Noting that the state $P|\Psi_\lambda^{(1)}\rangle$ satisfies the following equation:

$$(E_\lambda - \hat{H}_0)P|\Psi_\lambda^{(1)}\rangle = P\hat{V}\hat{J}P|\Psi_\lambda^{(1)}\rangle, \tag{9}$$

with the help of Eqs. (3a) and (4a) we can then write down the equation to be solved as

$$[\hat{J},\hat{H}_0]P = (E-\hat{H}_0)\hat{J}P - \hat{J}(E-\hat{H}_0)P = \hat{V}\hat{J}P - \hat{J}P\hat{V}\hat{J}P, \tag{10}$$

where we used Eqs. (1), (5), and (9). If we expand the operator $\hat{J}$ as

$$\hat{J} = \sum_{n=0}^{\infty} g^{(n)}\hat{J}^{(n)} = P + \sum_{n=1}^{\infty} g^{(n)}\hat{J}^{(n)}, \tag{11}$$

we have the following perturbative solutions in the order of $\hat{V}$:

$$\hat{J}^{(0)} = P, \quad \hat{J}^{(1)} = Q(E_P^0 - E_Q^0)^{-1}\hat{V}P, \ldots, \tag{12}$$

where E_P^0 and E_Q^0 are the eigenvalues of the unperturbed Hamiltonian $\hat{H}_0$ in P and Q space, respectively. Finally let us comment on the selection of a small number of bases in the P space, or construction of the projection operator P. Since we are mainly interested in the interaction potential between the atom and the probe tip, it is preferable to choose the bases so that the degrees of freedom of the subsystem (i) are eliminated. We assume, for simplicity, that eigenstates and eigenenergies of $\hat{H}_\alpha$ ($\alpha = A$ or B) are known as $|\alpha\rangle$, $|\alpha^*\rangle$, ..., and E_α^0, $E_{\alpha*}^0$ .... In addition, let the bath system, or the subsystem (i), be a set of excitons, photons, and their interactions, by assuming that the induced electric polarization in the macroscopic matter system is represented as excitons [23]. It is well known that such a system has characteristic elementary excitation modes, that is, exciton-polariton modes, or so-called ''dressed'' states of photons and excitons [24–26]. These eigenstates and eigenenergies are well determined. If we rewrite the photon operators in $\hat{\vec{D}}(\vec{r})$ [Eq. (8)] as exciton-polariton operators, we can obtain the bare interaction $\hat{V}$ in the exciton-polariton picture. Now let us choose a combination of the five states $|A\rangle$, $|A^*\rangle$, $|B\rangle$, $|B^*\rangle$, and $|0\rangle$ as the P-space bases. Here the ground state of $\hat{H}_{\text{bath}}$, including no exciton polaritons, is expressed as $|0\rangle$.

By using Eqs. (7a) and (12), the effective potential in the lowest order [27] can be written as

$$V_{\mathrm{eff}}(r)=-\frac{4\pi}{(2\pi)^3}\sum_{j=3}^{3}\sum_{\alpha\neq\alpha'}^{(A,B)}\int d^3k\left[\frac{K'_{\alpha}(\vec{k})K'^{*}_{\alpha'}(\vec{k})}{\Omega(\vec{k})-\Omega(\alpha')}+\frac{K'_{\alpha'}(\vec{k})K'^{*}_{\alpha}(\vec{k})}{\Omega(\vec{k})+\Omega(\alpha)}\right]. \tag{13}$$

Here the eigenenergy of the elementary excitation modes of the subsystem (i), that is, of the massive virtual photons, is denoted as $\hbar\Omega(k)$. The electronic excitation energies of the atom and the probe tip in the second subsystem are denoted as $E_A=\hbar\Omega(A)$ and $E_B=\hbar\Omega(B)$ ($\alpha,\alpha'=A$ or B). Note that the center-of-mass motion of the atom is not considered here. The coefficients $K'_{\alpha}(\vec{k})$ and its complex conjugate $K'^{*}_{\alpha}(\vec{k})$ represent the coupling strength of the elementary excitation modes to the atom and the probe tip, and one can obtain the explicit form of $K'_{\alpha}(\vec{k})$ to define the coupling coefficient $f(k)$ as

$$K'_{\alpha}(\vec{k})=\sum_{\lambda=1}^{2}\theta(z_{\alpha})\mu_{\alpha}[\vec{e}\cdot\vec{e}_{\lambda}(\vec{k})]f(k)e^{i\vec{k}\cdot\vec{r}_{\alpha}}, \tag{14a}$$

$$f(k)=\frac{ck}{\sqrt{\Omega(k)}}\frac{\sqrt{\Omega^2(k)-\Omega^2/4}}{\sqrt{2\Omega^2(k)-\Omega^2/4-c^2k^2}}, \tag{14b}$$

where the wave-number dependence of $f(k)$ characterizes a typical interaction range of exciton polaritons coupled to the subsystem (ii). Here the jth component of the dipole moment and the unit polarization vector for photons are, respectively, designated as $\mu_{\alpha}\vec{e}_j$ and $\vec{e}_{\lambda}(\vec{k})$. The quantities c and $E_{\mathrm{m}}=\hbar\Omega/2$ stand for the speed of light and the electronic excitation energy of the macroscopic matter in the subsystem (i).

On the basis of the dispersion relation of an exciton-polariton with effective mass m_p ($E_p=m_pc^2$), we perform the usual effective-mass approximation as follows:

$$\hbar\Omega(k)=\frac{\hbar\Omega}{2}+\frac{(\hbar k)^2}{2m_p}. \tag{15}$$

Substituting this expression into Eqs. (13), (14a), and (14b) we can rewrite the effective potential $V_{\mathrm{eff}}(r)$ as

$$\begin{aligned}V_{\mathrm{eff}}(r)&=-\frac{4\mu_A\mu_B\hbar E_p}{3i\pi r(\hbar c)^2}\int dkkf^2(k)e^{ikr}\left\{\frac{1}{k^2+2E_p(E_m+E_A)(\hbar c)^{-2}}+\frac{1}{k^2+2E_p(E_m-E_A)(\hbar c)^{-2}}\right.\\&\left.+\frac{1}{k^2+2E_p(E_m+E_B)(\hbar c)^{-2}}+\frac{1}{k^2+2E_p(E_m-E_B)(\hbar c)^{-2}}\right\}\\&=\frac{2\mu_A\mu_BE_p^2}{3i\pi r(\hbar c)^2}\int_{-\infty}^{\infty}dkkF(k)e^{ikr},\end{aligned} \tag{16}$$

where we average the summation over λ as 2/3, and define $F(k)$ as

$$F(k)\equiv\left(\frac{A_+}{k^2+\Delta_{A_+}^2}-\frac{A_-}{k^2+\Delta_{A_-}^2}\right)+\left(\frac{B_+}{k^2+\Delta_{B_+}^2}-\frac{B_-}{k^2+\Delta_{B_-}^2}\right)+\left(\frac{C_+}{k^2+\Delta_{C_+}^2}-\frac{C_-}{k^2+\Delta_{C_-}^2}\right). \tag{17}$$

Finally, as the sum of the Yukawa functions with several kinds of masses, we obtain the following near-field optical potential:

$$V_{\mathrm{eff}}(r)=\frac{2\mu_A\mu_BE_p^2}{3(\hbar c)^2}\{A_+Y(\Delta_{A_+}r)-A_-Y(\Delta_{A_-}r)+B_+Y(\Delta_{B_+}r)-B_-Y(\Delta_{B_-}r)\}, \tag{18a}$$

$$Y(\mu r)\equiv\frac{\exp(-\mu r)}{r}. \tag{18b}$$

The four kinds of effective masses of the Yukawa function are denoted as Δ_{A_+}, Δ_{B_+}, Δ_{A_-}, and Δ_{B_-}, of which the first two are heavier and thus have shorter interaction ranges. Two constants Δ_{C_+} and Δ_{C_-}, omitted in Eq. (18a), mainly give the periodic functions related to the property of the macroscopic matter, not the Yukawa function related to the microscopic subsystem. Here, we use the following explicit expression for the effective masses:

$$\Delta_{A_\pm}=\frac{\sqrt{2E_p(E_m\pm E_A)}}{\hbar c},\quad \Delta_{B_\pm}=\frac{\sqrt{2E_p(E_m\pm E_B)}}{\hbar c}, \tag{19}$$

assuming a blue detuning case [$\hbar\Omega(k)>E_m>E_A$ and E_B]. Note that the positive ones (Δ_{A_+} and Δ_{B_+}) are kept for a red detuning case [$E_m<\hbar\Omega(k)<E_A$ and E_B]. The first and second pairs of terms in Eq. (17) come from the coupling between the exciton polaritons and the subsystem (ii), while the third pair of terms originates from the macroscopic matter. The weight factors in Eq. (18a), that is, the numerators of each term in Eq. (17), are functions of E_A, E_B, E_p, and E_m.

Depending on whether the weight factor is positive or negative, it contributes to a repulsive or an attractive part of the effective potential $V_{\mathrm{eff}}(r)$.

III. PROPERTIES OF THE NEAR-FIELD OPTICAL POTENTIAL

Let us examine the features of the effective potential described by Eq. (18a). The potential is formally symmetric in terms of $A_{\pm}$ and $B_{\pm}$, and thus the discussion on one of the pairs is applicable to the other, though they are not necessarily the same in sign and magnitude. In the following, we will abbreviate $A_{\pm}$ or $B_{\pm}$ to $G_{\pm}$ unless otherwise stated. The sign and magnitude of $G_{\pm}$ depend on the detuning $\hbar\delta \equiv E_m - E_G$ and E_m. We consider a case where the detuning is large and the natural linewidth and saturation are negligible. The difference between G_+ and G_- is written as

$$G_+ - G_- \cong G_+ \left[1 - \frac{9}{5} \left(\frac{\hbar\delta}{E_m} + \frac{E_m}{2\hbar\delta} \right)^{-1} \right], \tag{20}$$

when $\hbar\delta$ stays between 0 and E_m in blue detuning. This detuning dependence is qualitatively consistent with that of the usual far-field optical potential in the large detuning limit [19,20]. Spontaneous emission and radiation pressure are also negligible in this limit [28]. If G_+ is positive, that is, blue detuned, and if the detuning $\hbar\delta$ is chosen so that the difference between G_+ and G_- is positive, the total potential then becomes repulsive, because the repulsive G_+ term is larger than the attractive G_- term. Note that the decay length of the repulsive G_+ term is shorter than that of the attractive G_- term.

As an example, we assume a typical alkali-metal atom with $E_{\mathrm{A}} = 1.6$ eV, where infrared and/or visible excitations of a macroscopic matter system and a probe tip are taken as $E_m = 1$–1.8 eV and $E_B = 1.0$–1.2 eV, respectively. Figure 2 represents several examples of the effective potentials. In Fig. 2(a) we use $E_A = 1.6$ eV, $E_B = 1.2$ eV, and $E_m = 1.0$ eV for a red-detuning case. Then G_+ is negative for red detuning and results in the attractive Yukawa potential. The solid line shows the total potential, while the dotted and dashed lines represent the attractive potentials with light and heavy effective masses, respectively. In contrast to red detuning, Fig. 2(b) shows a blue-detuning case, where we employ $E_A = 1.6$ eV, $E_B = 1.0$ eV, and $E_m = 1.8$ eV. This set of parameters leads to a repulsive potential for the $A_{\pm}$ term and an attractive potential for the $B_{\pm}$ term; the $(A_+ - A_-)$ term, in addition, is smaller than the $(B_+ - B_-)$ term; as a result, the attractive Yukawa potential occurs, as similar to Fig. 2(a). If a value of E_B is carefully chosen, it is possible to have a potential well for blue detuning. We show such an example in Fig. 2(c), where excitation energy of the probe tip is taken as $E_B = 1.2$ eV, while the other conditions are the same as in Fig. 2(b). In this case, the $(A_+ - A_-)$ term is larger than the $(B_+ - B_-)$ term, and thus the total potential forms a well as shown in the solid line. Figures 2(b) and 2(c) show how the difference in the balance between the $(A_+ - A_-)$ and $(B_+ - B_-)$ terms affects the final potential shapes.

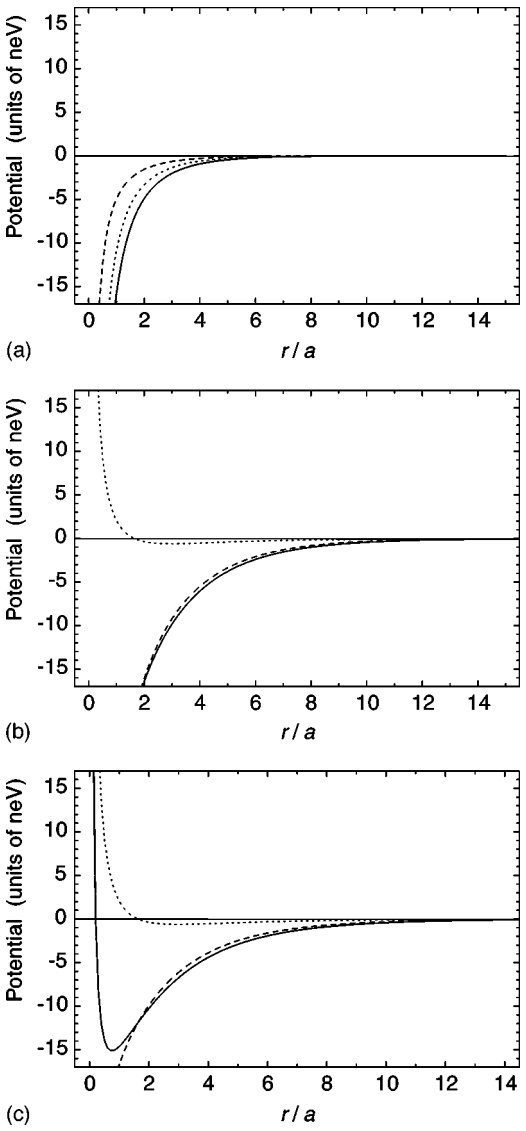

FIG. 2. Examples of the near-field optical potentials. (a) An attractive Yukawa potential in a red-detuning case. The resonance energy of an atom is assumed as $E_A = 1.6$ eV. The electronic excitation energies $E_B = 1.2$ eV and $E_m = 1.0$ eV are used for a probe tip and a macroscopic matter system, respectively. The solid line shows the total potential, while the dotted and dashed lines represent the attractive potentials with light and heavy masses. (b) An attractive Yukawa potential in a blue-detuning case. The excitation energies of the probe tip and the macroscopic matter system are chosen as $E_B = 1.0$ eV and $E_m = 1.8$ eV, respectively. The dotted, dashed, and solid lines represent the repulsive, attractive, and total potentials, respectively. (c) A potential well in a blue-detuning case. The excitation energy of the probe tip is chosen as $E_B = 1.2$ eV, while the other conditions are the same as in (b).

We can simply explain the detuning dependence of the near-field optical potential discussed above, on the basis of the wave-number dependence of the coupling coefficient $f(k)$ in Eq. (14b). It follows from Fig. 3 that $f(k)$ is constant when k is larger than the lower cutoff $k_c \approx 2\sqrt{m_p \Omega/\hbar} = 2\sqrt{2E_p E_m}/(\hbar c)$, while it is approximately proportional to k below k_c. The solid and dashed lines represent two cases

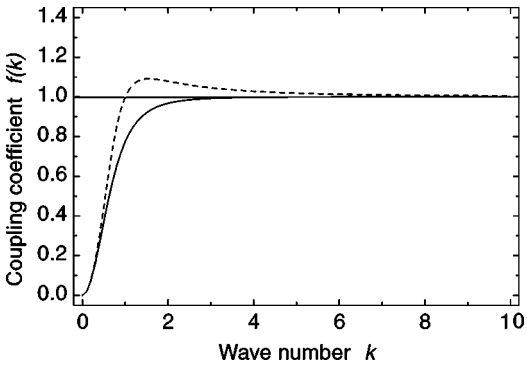

FIG. 3. Wave-number dependence of the coupling coefficient $f(k)$. The horizontal and vertical axes are measured in units of $\sqrt{E_m E_p}/\hbar c$ and $\sqrt{E_p}/\hbar$. The solid and dotted lines represent two cases of $E_p=E_m$ and $E_p=2E_m$, respectively.

of $E_p=E_m$ and $E_p=2E_m$, respectively. The coefficient $f(k)$ in the case of $E_p=E_m$ is always smaller than the asymptotic value, while in the case of $E_p=2E_m$ it becomes larger than the asymptotic value near the cutoff k_c. Simple estimation [29] yields $k_c \approx 1/100$ nm, which characterizes the interaction range of the exciton polaritons or massive virtual photons coupled to the subsystem (ii). It also shows that the coupling coefficient $f(k)$ is almost constant for a large red-detuning case and thus the Yukawa potential becomes attractive. For a blue-detuning case, the nonconstant term is not negligible and contributes to the repulsive potential.

As mentioned above, we can control the polarities and the interaction ranges of the Yukawa potentials, changing the detuning and material properties. It is thus possible to find the condition for forming a potential well due to the balance between the attractive and the repulsive potentials. Figure 4 illustrates such a condition. The solid curve shows how the weight factor of $B_- - B_+$ depends on the excitation energy E_B of a probe tip. The dashed line, which is independent of E_B, represents the weight factor $A_+ - A_-$ when the detuning and the resonance energies of both an atom and a macroscopic matter are fixed. The shaded area corresponds to the condition that the repulsive $A_+ - A_-$ term for blue detuning becomes larger than the attractive $B_+ - B_-$ term, that is, the condition that the total potential has a minimum. If we

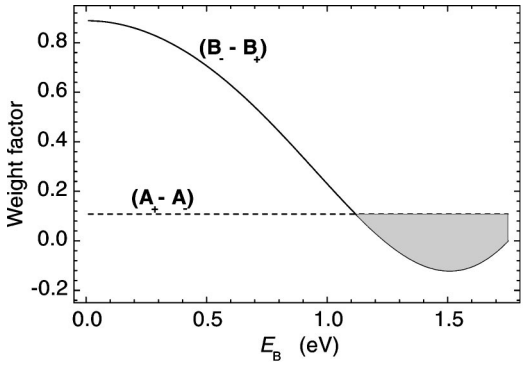

FIG. 4. Weight factor dependence on the excitation energy of a probe tip. If we take one of the excitation energies E_B in the shaded area, we can obtain a potential well as shown in Fig. 2(c).

choose a smaller value than $E_B=1.12$ eV, the smallest value in the shaded area, the $B_+ - B_-$ term becomes larger than the $(A_+ - A_-)$ term and the total potential results in an attractive Yukawa potential as shown in Fig. 2(b). Both Figs. 2 and 4 indicate that a near-field optical potential can have a minimum if we employ an appropriate detuning and material of a probe tip for the relevant system.

IV. NUMERICAL ANALYSIS

In the preceding sections we microscopically described the near-field optical potential as the sum of the Yukawa functions with several kinds of effective masses, and discussed the fundamental features of the potential. As an example of the application of the near-field optical potential, let us consider two cases of single-atom manipulation using optical near fields generated by a nanometric probe tip: (1) atom deflection, where an atom is cooled down on the order of millikelvins, and (2) atom trapping, where an atom is further cooled down on the order of microkelvins. Our intention is to provide an experimental guideline as well as to deepen the physical understanding of optical near fields and related phenomena. The cases considered involve experimentally unique techniques that will be essential for carrying an atom to a desired point on a substrate with high spatial accuracy far beyond the diffraction limit.

In order to take the size of a probe-tip sphere explicitly into account, we simply integrate $V_{\rm eff}(r)$ in Eq. (18a) within the sphere (variable radius: a) as

$$V(r)=\frac{1}{4\pi a^3/3}\int V_{\rm eff}(|\vec{r}_A-(\vec{r}'+\vec{r}_B)|)d^3r'$$
$$=\frac{\mu_A\mu_B E_P^2}{(\hbar c)^2 a^3}\left[\sum_{G,j=\pm}\frac{jG_j}{\Delta_{Gj}^3}\{(1+a\Delta_{Gj})\right.$$
$$\left.\times\exp(-\Delta_{Gj}a)-(1-a\Delta_{Gj})\exp(\Delta_{Gj}a)\}Y(\Delta_{Gj}r)\right], \tag{21}$$

redefining the argument r of the potential V as $r=|\vec{r}|=|\vec{r}_A-\vec{r}_B|$. Thus the total potential $V(r)$ is expressed as a function of the distance between the center of the tip sphere and the atomic center. Here we assume that the atom is pointlike with discrete energy levels, while the Yukawa sources are homogeneously distributed within the probe-tip sphere [30]. The total potential $V(r)$ is used in the following simulation of atom deflection and trapping. As a test case, let us use a ^{85}Rb atom with $E_A=1.59$ eV and $\mu_A=7.5$ debye. For the effective mass of the exciton polaritons, $E_p=m_pc^2=\hbar\Omega$ is employed.

First we discuss Rb-atom deflection by the effective potential $V(r)$. It is formulated as a potential scattering problem in the first Born approximation. As the velocity of the atom decreases, the first Born approximation becomes invalid. It is known, however, that the breakdown of the first Born approximation occurs when the incident velocity is

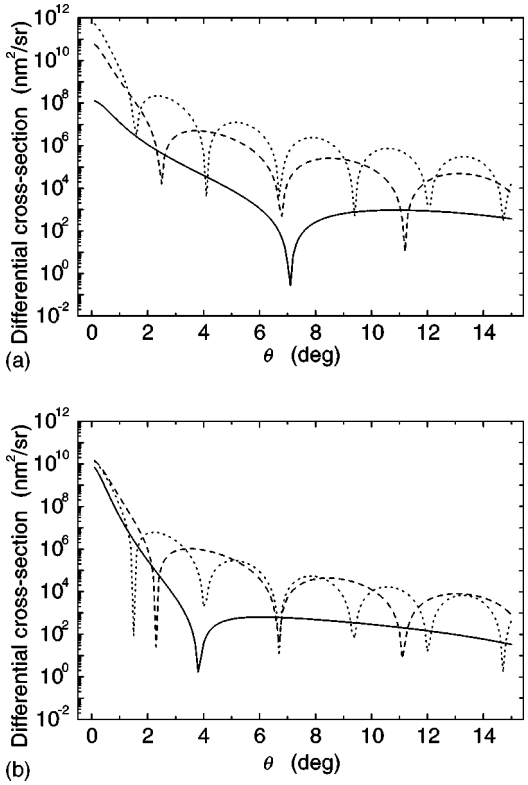

FIG. 5. Differential scattering cross section of ^{85}Rb with an incident velocity of 1 m/s in the first Born approximation. The near-field optical potential is generated by a probe tip with a radius of 10–50 nm for (a) a red-detuning case and (b) a blue-detuning case. Solid: $a=10$ nm; dashed: $a=30$ nm; and dotted: $a=50$ nm.

close to the sub-meter-per-second range or the kinetic energy is in the submillikelvin range [29]. Figure 5 represents the differential scattering cross section, or angular distribution of ^{85}Rb with an incident velocity of 1 m/s, or 10 mK in terms of temperature, as the radius a of the probe tip varies from 10 to 50 nm. The solid, dashed, and dotted lines show the results for $a=10$ nm, $a=30$ nm, and $a=50$ nm, respectively. Figure 5(a) is calculated with the red-detuned potential similar to that in Fig. 2(a), while Fig. 5(b) is calculated with the blue-detuned potential similar to that in Fig. 2(c). The periodic structure seen in the figures results from the finite size of the probe tip. From the analytic expression it follows that the periodic length is inversely proportional to the tip size: the larger the tip size is, the shorter the period is. Both figures show that a smaller probe tip can deflect the atom more strongly, though an optimum size should be determined from a discussion on the de Broglie wavelength of the atom. The difference between Figs. 5(a) and 5(b) can be understood as follows: In Fig. 5(a), two components with the same signs of the effective potential $V(r)$ constructively contribute to the scattering amplitude, $\int r \sin(qr)V(r)dr$, where q is the transferred momentum. On the other hand, in Fig. 5(b), two components with opposite signs of $V(r)$, the repulsive and attractive, are destructively summed up in the scattering amplitude. This reduces the deflection angle θ in Fig. 5(b) in comparison with those in Fig. 5(a).

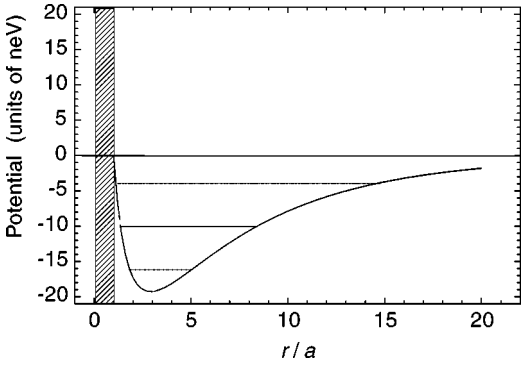

FIG. 6. Example of near-field optical potential for ^{85}Rb (resonance energy of 1.59 eV), represented by the solid line. The probe tip is assumed to have a radius of 10 nm and an electronic excitation energy of 1.51 eV. The probe tip and atom system is coupled with a macroscopic matter system with $E_m=2.0$ eV. Approximating it by a harmonic-oscillator potential around the minimum point, vibrational levels with the labels $n=0$, 1, and 2 are shown. The shaded area shows the probe-tip size.

Next let us consider an example of a near-field optical potential for atom trapping. Figure 6 shows a case for the system of a ^{85}Rb atom with an excitation energy $E_A=1.59$ eV and a probe tip with a radius $a=10$ nm, a transition dipole moment $\mu_B=1.5$ debye, and an excitation energy $E_B=1.51$ eV. They are coupled with a macroscopic matter with $E_m=2.0$ eV. In order to determine the value of the excitation energy E_B, we perform a similar analysis developed in Fig. 4 by means of the total potential $V(r)$. As a result, the smallest value of 1.51 eV is chosen from the possible values giving a potential well in the case of $a=10$ nm. This condition would be satisfied if we choose, for example, a III-V compound of $Al_xGa_{1-x}As$. It follows from Fig. 6 that the potential has a minimum, -20 neV, near the position $r=2a$ from the probe-tip surface. Approximating it by a harmonic-oscillator potential around the minimum point, we find that two or three vibrational levels can be supported; the lowest vibrational energy with the label $n=0$ corresponds to 3.1 neV, or equivalently 35 μK. This result suggests the possibility of a single Rb-atom trapping at this level.

It may be interesting to compare the depth of the above potential well with the ones obtained for an atom and a microsphere system, where the radius of the sphere is much larger than ours. The potential depth for a Rb atom semiclassically calculated in Ref. [31] is the same order of magnitude, or a little shallower, as our results. However, their minimum position of the potential depends on the wavelength used and is different from ours. This is because they use a microsphere with a dielectric constant of 6 and a radius of about 1 μm for visible light. The potential for a Cs atom quantum-mechanically calculated with a 50-μm sphere shows the similar tendency [32]. It follows that the nonresonant term neglected in Ref. [31], which is the optical near field leading to the size-dependent effect, becomes important as a tip sphere becomes smaller. The effect of an ideally conducting conical surface on an atom was also classically estimated [33], and an energy shift of the atom in the region

of interest seems to be a similar order of magnitude though the details of the parameters used are not known.

V. CONCLUSIONS

We have microscopically derived an effective interaction potential between a neutral atom and a nanometric probe tip in optical near-field systems. The near-field optical potential consists of the sum of the Yukawa functions with several kinds of effective masses, which is attractive or repulsive, depending on the detuning and material properties. This approach succeeds in quantitatively analyzing the probe-tip size and material dependence of the potential. It also can be applied to a variety of phenomena inherent to optical near-field techniques.

Recent experiments in atom manipulation and nanostructure fabrication [34] have made remarkable progress. An atomic mirror [35–37] and an atomic guide with a hollow fiber and blue-detuned optical near field [38,39] have been experimentally demonstrated. An atomic guide using magnetic forces has been recently reported [40,41]. A beam of laser-cooled atoms was also guided by a pair of parallel wires produced on a glass substrate by photolithography and subsequent electroplating [42]. In addition to these methods, atom deflection and trapping with a nanometric tip will greatly advance the manipulation techniques. In fact, we have shown the possibilities of such atom deflection and trapping. These analyses also illustrate the usefulness of the microscopic theory developed in this paper. The probe-tip size and potential shape are quantitatively shown as key parameters of atom deflection. The difference in the deflection angles for the attractive and the repulsive potentials is explained by the Yukawa potentials with two kinds of effective masses. Besides, by choosing appropriate detuning and material properties, it is numerically shown that a potential well is generated to be suitable for Rb-atom trapping. It means that we can form a well in the near-field optical potential with single blue-detuned light, though the methods based on the existing far-field theories mentioned in Sec. I require both red- and blue-detuned laser beams. Moreover, we expect that we can apply the near-field optical potential method to atom deposition [43] and nanostructure fabrication. These microscopic analyses will provide useful information for the future experimental demonstration.

[1] M. Ohtsu, K. Kobayashi, H. Ito, and G.H. Lee, Proc. IEEE **88**, 1499 (2000).

[2] *Near-Field Nano/Atom Optics and Technology*, edited by M. Ohtsu (Springer-Verlag, Berlin, 1998).

[3] T. Yatsui, M. Kourogi, and M. Ohtsu, Appl. Phys. Lett. **73**, 2090 (1998).

[4] T. Saiki and K. Matsuda, Appl. Phys. Lett. **74**, 2773 (1999).

[5] Y. Toda, S. Shinomori, K. Suzuki, and Y. Arakawa, Appl. Phys. Lett. **73**, 517 (1998).

[6] T. Matsumoto, M. Ohtsu, K. Matsuda, T. Saiki, H. Saito, and K. Nishi, Appl. Phys. Lett. **75**, 3246 (1999).

[7] V.V. Polonski, Y. Yamamoto, M. Kourogi, H. Fukuda, and M. Ohtsu, J. Microsc. **194**, 545 (1999).

[8] Y. Yamamoto, M. Kourogi, M. Ohtsu, V. Polonski, and G.H. Lee, Appl. Phys. Lett. **76**, 2173 (2000).

[9] H. Hori, in *Near Field Optics*, edited by D.W. Pohl and D. Courjon (Kluwer, Dordrecht, 1993), pp. 105–114.

[10] M. Ohtsu, S. Jiang, T. Pangaribuan, and M. Kozuma, in *Near Field Optics*, edited by D.W. Pohl and D. Courjon (Kluwer, Dordrecht, 1993), pp. 131–139.

[11] M. Ohtsu and H. Hori, *Near-Field Nano-Optics* (Kluwer/Plenum, New York, 1999).

[12] C. Girard, O.J.F. Martin, and A. Dereux, Phys. Rev. Lett. **75**, 3098 (1995).

[13] K. Cho, Y. Ohfuti, and K. Arima, Surf. Sci. **363**, 378 (1996).

[14] O. Keller, Ultramicroscopy **71**, 1 (1998).

[15] K. Kobayashi, Appl. Phys. A: Mater. Sci. Process. **66**, S391 (1998).

[16] K. Kobayashi and M. Ohtsu, J. Microsc. **194**, 249 (1999), and references therein.

[17] Yu.B. Ovchinnikov, S.V. Shul'ga, and V.I. Balykin, J. Phys. B **24**, 3173 (1991).

[18] H. Mabuchi and H.J. Kimble, Opt. Lett. **19**, 749 (1994).

[19] J.P. Dowling and J. Gea-Banacloche, in *Advances in Atomic, Molecular, and Optical Physics*, edited by B. Bederson and H. Walther (Academic Press, San Diego, 1996), Vol. 37.

[20] J. Dalibard and C. Cohen-Tannoudji, J. Opt. Soc. Am. B **2**, 1707 (1985).

[21] C. Cohen-Tannoudji, *Atoms in Electromagnetic Fields* (World Scientific, Singapore, 1994).

[22] D.P. Craig and T. Thirunamachandran, *Molecular Quantum Electrodynamics* (Dover, New York, 1998).

[23] H. Haken, *Quantum Field Theory of Solids* (Elsevier, Amsterdam, 1983).

[24] J.J. Hopfield, Phys. Rev. **112**, 1555 (1958).

[25] J. Knoester and S. Mukamel, Phys. Rev. A **40**, 7065 (1989).

[26] B. Huttner and S.M. Barnett, Phys. Rev. A **46**, 4306 (1992).

[27] Since we are primarily interested in interactions between a neutral atom and a nanometric probe tip originated from optical near fields, we assume the situation that the neutral atom interacts with the probe tip only if incident light comes into a macroscopic matter system. In other words, of *P*-space bases, we employ eigenstates of an unperturbed Hamiltonian, where the neutral atom and the probe tip are isolated from each other. If one is interested in atomic interactions between a neutral atom and probe-tip atoms as well as optical near-field interactions, one can use appropriate eigenstates of an unperturbed Hamiltonian, including such interactions as *P*-space bases.

[28] G. Grynberg, B. Lounis, P. Verkerk, J.-Y. Courtois, and C. Salomon, Phys. Rev. Lett. **70**, 2249 (1993).

[29] K. Kobayashi, S. Sangu, H. Ito, and M. Ohtsu, in *Near-Field Optics: Principles and Applications*, edited by X. Zhu and M. Ohtsu (World Scientific, Singapore, 2000).

[30] In Sec. II we assume that we know eigenstates of a probe tip when it is isolated, for example, confined states in a sphere with a radius of *a*. Then the effective interaction potential be-

tween two arbitrary points with energy levels (one is located in the probe tip and the other is located at the center of the neutral atom) is derived as Eq. (18a). If we assume that the tip is made up of such linearly independent points, then the total potential is given as an integration of Eq. (18a) over the sphere.

[31] V. Klimov, V.S. Letokhov, and M. Ducloy, Eur. Phys. J. D **5**, 345 (1999).

[32] D.W. Vernooy and H.J. Kimble, Phys. Rev. A **55**, 1239 (1997).

[33] V.V. Klimov and Ya.A. Perventsev, Quantum Electron. **29**, 847 (1999).

[34] W.R. Anderson, C.C. Bradley, J.J. McClelland, and R.J. Celotta, Phys. Rev. A **59**, 2476 (1999).

[35] V.I. Balykin, V.S. Letokhov, Yu.B. Ovchinnikov, and A.I. Sidorov, Phys. Rev. Lett. **60**, 2137 (1988).

[36] C.G. Aminoff, A.M. Steane, P. Bouyer, P. Desbiolles, J. Dalibard, and C. Cohen-Tannoudji, Phys. Rev. Lett. **71**, 3083 (1993).

[37] A. Landragin, J.-Y. Courtois, G. Labeyrie, N. Vansteenkiste, C.I. Westbrook, and A. Aspect, Phys. Rev. Lett. **77**, 1464 (1996).

[38] M.J. Renn, E.A. Donley, E.A. Cornell, C.E. Wieman, and D.Z. Anderson, Phys. Rev. A **53**, R648 (1996).

[39] H. Ito, T. Nakata, K. Sakaki, M. Ohtsu, K.I. Lee, and W. Jhe, Phys. Rev. Lett. **76**, 4500 (1996).

[40] E.A. Hinds, M.G. Boshier, and I.G. Hughes, Phys. Rev. Lett. **80**, 645 (1998).

[41] J. Denschlag, D. Cassettari, and J. Schmiedmayer, Phys. Rev. Lett. **82**, 2014 (1999).

[42] D. Müller, D.Z. Anderson, R.J. Grow, P.D.D. Schwindt, and E.A. Cornell, Phys. Rev. Lett. **83**, 5194 (1999).

[43] H. Ito, K. Sakaki, M. Ohtsu, and W. Jhe, Appl. Phys. Lett. **70**, 2496 (1997).